

# Physical and orbital properties of the stellar system HIP 43766

Hatem Widyan and Hussam Aljboor

Department of Physics, Al al-Bayt University, Mafraq 25113, Jordan; [widyan@aabu.edu.jo](mailto:widyan@aabu.edu.jo)

Received 2020 October 12; accepted 2020 November 24

**Abstract** In this paper, we present the analysis of the stellar binary system HIP 43766 to determine its properties. We rely on dynamical modeling and atmospheric modeling with recent data to determine the orbital solution and the physical properties of the system. There is a consistency between observed and synthetic photometry obtained using atmospheric modeling. The calculated dynamical mass sum of the system ranged between 1.691 and 2.609 solar masses, while it ranges between 2.0 and 2.1 as estimated utilizing atmospheric modeling. This could be due to inaccuracy in estimating the orbit, which could be modified with future observations with more relative positional measurements. The parameters of the system and the position of the components on the evolutionary tracks show that the system consists of F5 and G5 subgiant stars, mostly formed by fragmentation. A dynamical mass sum is predicted for the system.

**Key words:** stars: binaries: close — stars: binaries: visual — stars: individual: HIP 43766

## 1 INTRODUCTION

It is well known that most of the stars in the sky are binary or multiple systems (Duquennoy & Mayor 1992). To determine the physical and geometrical parameters of a binary system, one should analyze these systems. Moreover, the most accurate and reliable method for estimating stellar masses is by analyzing stellar binary systems. Binary systems play many roles in astrophysics. For example, they are used to examine the formation of stars and stellar evolutionary theories. Sometimes, high resolution observational techniques such as speckle interferometry (e.g., Labeyrie 1970 and Balega & Tikhonov 1977) and adaptive optics are not sufficient to determine the physical parameters of the individual components of visual close binary systems (VCBS). However, a photodynamical model can be adopted for an eclipsing binary system (e.g., Sürgit et al. 2020).

In 2002, Al-Wardat (2002) introduced a new method for estimating the physical and geometrical parameters of both components of VCBS by combining spectrophotometry with atmospheric modeling. In order to be able to employ this novel method, one must determine the magnitude differences which are obtained from speckle interferometry measurements, as well as the color indices. This new method along with the dynamical modeling developed by Tokovinin (1992) has been applied to many systems (e.g., Al-Wardat et al. 2014a; Al-Wardat et al. 2014b; Al-Wardat et al. 2014c; Al-Wardat et al. 2016;

Al-Wardat et al. 2017; Masda et al. 2018; Masda et al. 2019b and Masda et al. 2019a).

In Table 1, we present basic information on the HIP 43766 system. Note that the system has three different values for parallax. The first parallax of the system is obtained from the Hipparcos and Tycho Catalogues and its value is  $21.70 \pm 1.32$  mas, which corresponds to a distance of  $d = 46.08$  pc. The second value is referenced from the Hipparcos New Astrometric Catalog (Van Leeuwen 2007) and its value is  $20.40 \pm 0.92$  mas, which corresponds to a distance of  $48.85 \pm 0.05$  pc, while the third value is acquired from the Gaia Data Release 2 and its value is  $23.04135 \pm 1.1074$ , which corresponds to a distance of  $d = 43.46$  pc.

The paper is organized as the follows. In Section 2, we present the orbital analysis of the system. In Section 3, the physical properties of individual stars in the system are determined. Results and discussion are presented in Section 4. Finally, we provide the conclusion of our findings in Section 5.

## 2 ORBITAL SOLUTION

The dynamical modeling technique developed by Tokovinin (2016) is employed to estimate the orbital properties of HIP 43766: the period ( $P$ ), epoch of passage through periastron ( $T_0$ ), eccentricity ( $e$ ), semi-major axis ( $a$ ), inclination ( $i$ ), longitude of periastron ( $\omega$ ) and position angle of the line of nodes ( $\Omega$ ) for the stellar system. To

**Table 1** Fundamental Parameters and Observed Photometric Data for HIP 43766

Property	Parameter	Value	Reference
Position	$\alpha_{2000}$	08 <sup>h</sup> 54 <sup>m</sup> 55 <sup>s</sup> .98	<a href="http://simbad.u-strasbg.fr/simbad">http://simbad.u-strasbg.fr/simbad</a> SIMBAD
	$\delta_{2000}$	+26°11'53.84	<a href="http://simbad.u-strasbg.fr/simbad">http://simbad.u-strasbg.fr/simbad</a> SIMBAD
Magnitude [mag]	$m_v$	6.73	ESA (1997)
	$m_b$	7.385	ESA (1997)
	$(B - V)_J$	0.65 ± 0.009	ESA (1997)
	$A_v$	0.006	Lallement et al. (2014)
	$B_T$	7.522 ± 0.008	Høg et al. (2000)
	$V_T$	6.817 ± 0.007	Høg et al. (2000)
	$(B - T)_T$	0.657 ± 0.008	Høg et al. (2000)
Parallax [mas]	$\pi_{\text{Hip}}$	21.70 ± 1.32	ESA (1997)
	$\pi_{\text{Hip}}$	20.40 ± 0.92	Van Leeuwen (2007)
	$\pi_{\text{Gaia}}$	23.04135 ± 1.1074	Gaia <sup>1</sup>

<sup>1</sup>Collaboration et al. (2018).**Table 2** The latest relative positional measurements for the HIP 43766 system taken from the Fourth Catalog of Interferometric Measurements of Binary Stars.

Epoch	Theta ( $\theta^\circ$ )	Rho ( $\rho''$ )	Reference
1976.8579	142.7	0.23	McAlister (1978)
1976.9234	143.2	0.239	McAlister & DeGioia (1979)
1978.1493	154.5	0.279	McAlister (1980)
1980.1563	168.9	0.336	McAlister et al. (1983)
1980.907	171.6	0.33	Tokovinin (1982)
1982.2888	178.9	0.367	Fu et al. (1997)
1982.847	183	0.387	Tokovinin (1983)
1983.0479	183.5	0.373	McAlister et al. (1987)
1984.0553	187.8	0.378	McAlister et al. (1987)
1984.9312	192	0.401	Bonneau et al. (1986)
1985.0001	192	0.382	McAlister et al. (1987)
1986.8839	200.3	0.394	McAlister et al. (1989)
1987.269	201.3	0.392	Hartkopf et al. (2000)
1989.2296	209.1	0.395	McAlister et al. (1990)
1990.2699	213.7	0.398	Hartkopf et al. (1992)
1991.25	217	0.392	ESA (1997)
1991.3184	217.5	0.394	Hartkopf et al. (1994)
1991.68	232.8	0.44	Fabrizius et al. (2002)
1991.8944	219.7	0.395	Hartkopf et al. (1994)
1992.3068	221.1	0.393	Hartkopf et al. (1994)
1993.9259	228.1	0.384	Hartkopf et al. (1997)
1994.0927	228.9	0.393	Hartkopf et al. (1997)
1995.1492	233.6	0.382	Hartkopf et al. (1997)
1995.9191	235.1	0.383	Hartkopf et al. (1997)
1996.8663	240.1	0.377	Hartkopf et al. (2000)
1997.1315	241.2	0.37	Hartkopf et al. (2000)
2001.02	259.1	0.366	Mason et al. (2011)
2005.8636	281.2	0.353	Mason et al. (2011)
2006.0548	283.1	0.36	Roberts Jr & Mason (2017)
2008.101	293.8	0.348	Gili & Prieur (2012)

estimate these elements, we rely on relative position measurements from speckle interferometric observations.

The method requires initial values of the positional measurements of the system, which are obtained from the Fourth Catalog of Interferometric Measurements of Binary Stars and from Mason et al. (2018). We input these values in the ORBITX code (Tokovinin 1992) to determine the best-fit orbit for the system.

The relative positional measurements of the system are listed in Table 2. The orbit of the system was built by Mason (2000). Mason used the first 26 points measured before 2000 to construct the orbit. We have included four new points to modify the orbit and to estimate

**Table 3** Modified Orbital Parameters of the HIP 43766 System along with the Previous One

Parameter	Unit	This work	Mason (2000)
$P \pm \sigma_P$	[yr]	45.9506 ± 0.3513	45.02
$T_0 \pm \sigma_{T_0}$	[yr]	1973.3197 ± 0.059	1973.16
$e \pm \sigma_e$		0.4896 ± 0.0077	0.475
$a \pm \sigma_a$	[arcsec]	0.3603 ± 0.0009	0.347
$i \pm \sigma_i$	[deg]	45.5 ± 0.31	43.5
$\Omega \pm \sigma_\Omega$	[deg]	159.63 ± 0.84	162.1
$\omega \pm \sigma_\omega$	[deg]	261.71 ± 0.3	257.5
rms( $\theta$ )	[deg]	0.52	–
rms( $\rho$ )	[arcsec]	0.0031	–

**Table 4** Dynamical Mass of HIP 43766

	Dynamical Mass	
	Mason (2000) ( $M_\odot$ )	This work ( $M_\odot$ )
$\pi_{\text{Hip1997}}$	2.017	2.168 ± 0.397
$\pi_{\text{Hip2007}}$	2.428	2.609 ± 0.356
$\pi_{\text{Gaia2018}}$	1.691	1.817 ± 0.264

the new orbital parameters. The estimated new orbital parameters of the system and the old values are listed in Table 3. Figure 1 displays the relative visual orbit of the system with the epoch of the positional measurement while Figure 2 depicts the new orbit against the old one obtained earlier by Mason (2000).

We have calculated the total dynamical mass with relatively small values of errors in this binary system via Kepler's third law. The total dynamical mass is given by

$$M_{Tot.} = M_A + M_B = \left( \frac{a^3}{\pi^3 P^2} \right) M_\odot, \quad (1)$$

where  $M_B$  is the mass of the primary component,  $M_B$  is the mass of the secondary component,  $a$  is the semi-major axis in arcseconds,  $\pi$  is the parallax in arcseconds and  $P$  is the period in years.

The formal error in the mass is

$$\frac{\sigma_M}{M} = \sqrt{9\left(\frac{\sigma_\pi}{\pi}\right)^2 + 9\left(\frac{\sigma_a}{a}\right)^2 + 4\left(\frac{\sigma_P}{P}\right)^2}. \quad (2)$$

Using the values of  $a$  and  $P$  obtained from the orbital solution and the three values of parallax measurement, we estimate the dynamical mass. Table 4 lists the comparison

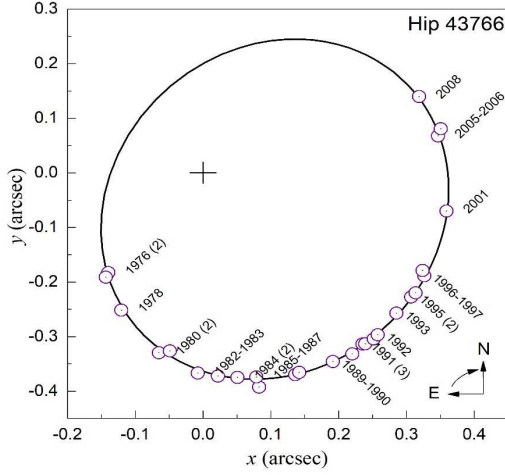


**Fig. 1** The relative visual orbit of the system with the epoch of the positional measurement.

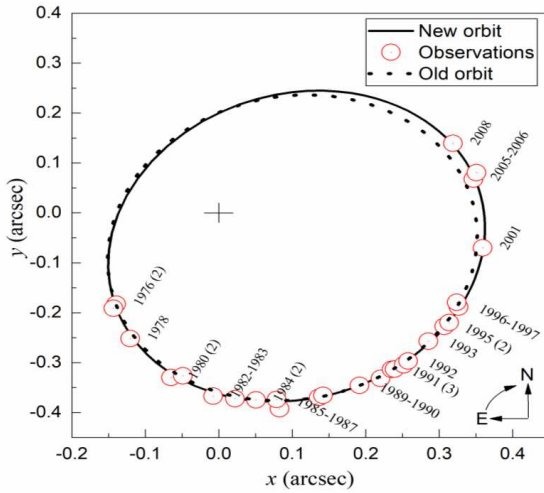


**Fig. 2** The difference in the orbit between the last work from Mason (2000) and this work.

between dynamical masses obtained from the Mason (2000) work and this work.

### 3 PHYSICAL ELEMENTS

We employ a novel technique from Al-Wardat (2002) to estimate the physical properties of each star in the system; i.e., the effective temperatures ( $T_{\text{eff}}$ ), radii ( $R$ ), gravitational accelerations ( $\log g$ ), luminosities ( $L$ ) masses and spectral types ( $S_p$ ).

The technique is based on building individual spectral energy distribution (SED) models for the system's components. To do so, we first calculate the average of  $\Delta m$  measurements in the  $V$ -band from the speckle interferometric results (Table 5). The average value calculated from these measurements is given by  $\Delta m = 1.686$ .

We then used this value of  $\Delta m$  along with the visual magnitude of the system listed in Table 1; i.e.,  $m_v = 6.73$ , in the following equations to get the apparent magnitudes for the two main components of the system; i.e., components  $A$  and  $B$

$$m_v^A = m_v + 2.5 \log (1 + 10^{-0.4\Delta m}), \quad (3)$$

$$m_v^B = m_v^A + \Delta m. \quad (4)$$

Also, the absolute magnitude of the two components of the system is calculated from the following equation

$$M_V = m_v + 5 - 5 \log d - A_V, \quad (5)$$

where  $A_V$  is the interstellar extinction coefficient and its value is 0.006. By considering the values of the absolute magnitudes for each component in the system, we are able to fix the values of effective temperature, bolometric correction ( $B.C.$ ), mass and spectral type for each component in our system from the tables listed in Gray (2005) and Lang (1992).

The preliminary values of bolometric magnitude ( $M_{\text{bol}}$ ), luminosity ( $L$ ), radius ( $R$ ) and gravitational acceleration ( $\log g$ ) for the two main components of the system are calculated utilizing the following well-known equations for a main sequence star:

$$M_{\text{bol}} = M_V + B.C., \quad (6)$$

$$\log \frac{L}{L_{\odot}} = \frac{M_{\text{bol}}^{\odot} - M_{\text{bol}}}{2.5}, \quad (7)$$

$$\log \left( \frac{R}{R_{\odot}} \right) = 0.5 \log \left( \frac{L}{L_{\odot}} \right) - 2 \log \left( \frac{T_{\text{eff}}}{T_{\text{eff}_{\odot}}} \right), \quad (8)$$

$$\log g = \log \left( \frac{M}{M_{\odot}} \right) - 2 \log \left( \frac{R}{R_{\odot}} \right) + 4.43, \quad (9)$$

where  $T_{\odot} = 5777$  K,  $R_{\odot} = 6.69 \times 10^8$  m and  $M_{\text{bol}}^{\odot} = 4^m.75$ .

The preliminary specific values of the physical parameters for the components of the system for each parallax are listed in Table 6.

Next, we use these estimated values in Table 6 as preliminary input parameters for the grids of Kurucz's line-blanketed plane-parallel models (ATLAS9) to obtain preliminary synthetic SEDs for stars  $A$  and  $B$  for each value of the parallax. These are then combined to get the total synthetic SED of the system according to the following equation (Al-Wardat 2012)

$$F_{\lambda} \cdot d^2 = H_{\lambda}^A \cdot R_A^2 + H_{\lambda}^B \cdot R_B^2, \quad (10)$$

which can be written as

$$F_{\lambda} = \left( \frac{R_A}{d} \right)^2 \left( H_{\lambda}^A + H_{\lambda}^B \cdot \left( \frac{R_A}{R_B} \right)^2 \right), \quad (11)$$

where  $H_{\lambda}^A$  and  $H_{\lambda}^B$  represent the flux from a unit surface of the system's components  $A$  and  $B$ , respectively, and  $F_{\lambda}$  signifies the total SED of the entire system.

**Table 5** Magnitude Difference between the Two Components of the HIP 43766 System in Different Filters in the Visual Band

$\Delta m$ (mag)	$\sigma_{\Delta m}$ (mag)	Filter ( $\lambda/\Delta\lambda$ ) (nm)	Telescope diameter (m)	Reference
1.505	0.015	511/222	0.3	ESA (1997)
1.49	0.01	505/97	3.5	Fabricius & Makarov (2000)
2.07	0.01	530/100	1.4	Fabricius et al. (2002)

**Table 6** Preliminary Physical and Geometrical Properties of Each Star in the HIP 43766 System

Parameter	Unit	1		2		3	
		Comp. A	Comp. B	Comp. A	Comp. B	Comp. A	Comp. B
$m_v$	[mag]	6.93843	8.62443	6.93843	8.62443	6.93843	8.62443
$M_V$	[mag]	3.61487	5.30087	3.48811	5.17411	3.74199	5.42799
$M_{\text{bol}}$	[mag]	3.50487	4.99087	3.34811	4.96411	3.59199	5.11799
$T_{\text{eff}}$	[K]	6890	5635	6440	5770	6280	5635
$R$	[ $R_{\odot}$ ]	1.24736	0.940681	1.53465	0.908303	1.44241	0.887196
$L$	[ $L_{\odot}$ ]	3.14812	0.801034	3.6371	0.821023	2.9054	0.712534
Log $g$	[cgs]	4.41986	4.42163	4.20411	4.47733	4.21219	4.47248
$M$	[ $M_{\odot}$ ]	1.52	0.87	1.4	0.92	1.26	0.87
Sp. Type		F2	G7	F5	G5	F7	G7

<sup>1</sup> using old Hipparcos parallax (ESA 1997) ( $\pi \pm \sigma_{\pi} = 21.70 \pm 1.32$ ); <sup>2</sup> using new Hipparcos parallax (Van Leeuwen 2007) ( $\pi \pm \sigma_{\pi} = 20.40 \pm 0.92$ ); <sup>3</sup> using Gaia parallax (Collaboration et al. 2018) ( $\pi \pm \sigma_{\pi} = 23.04135 \pm 1.107$ ).

**Table 7** Estimated Physical Parameters of Individual Components in the HIP 43766 System for the Three Parallax Measurements

Parameter	Unit	1		2		3	
		Comp. A	Comp. B	Comp. A	Comp. B	Comp. A	Comp. B
$M_V$	[mag]	3.36	4.95	3.23	4.82	3.48	5.09
$M_{\text{bol}}$	[mag]	3.24	4.76	3.11	4.62	3.36	4.91
$T_{\text{eff}}$	[K]	6010	5350	6010	5350	6010	5350
$R$	[ $R_{\odot}$ ]	1.852	1.163	1.971	1.253	1.751	1.085
$M$	[ $M_{\odot}$ ]	1.21	0.85	1.253	0.85	1.18	0.82
Log $g$	[cgs]	4.5	4.55	4.50	4.55	4.50	4.55
Sp. Type		F4IV	G4IV	F3IV	G3IV	F5IV	G5IV

<sup>1</sup> using old Hipparcos parallax (ESA 1997) ( $\pi \pm \sigma_{\pi} = 21.70 \pm 1.32$ ); <sup>2</sup> using new Hipparcos parallax (Van Leeuwen 2007) ( $\pi \pm \sigma_{\pi} = 20.40 \pm 0.92$ ); <sup>3</sup> using Gaia parallax (Collaboration et al. 2018) ( $\pi \pm \sigma_{\pi} = 23.04135 \pm 1.107$ ).

**Table 8** Magnitudes and Color Indices of the Entire Synthetic Spectrum and Individual Components of HIP 43766

System	Filter	$\pi_{\text{Hip1997}}$			$\pi_{\text{Hip2007}}$			$\pi_{\text{Gaia2018}}$		
		Entire Synth. $\sigma = \pm 0.03$	A	B	Entire Synth. $\sigma = \pm 0.03$	A	B	Entire Synth. $\sigma = \pm 0.03$	A	B
Joh-Cou.	$U$	7.55	7.68	9.90	7.55	7.68	9.90	7.55	7.68	9.92
	$B$	7.39	7.56	9.45	7.39	7.56	9.46	7.39	7.56	7.48
	$V$	6.73	6.94	8.62	6.73	6.94	8.62	6.73	6.94	8.62
	$R$	6.37	6.60	8.17	6.37	6.60	8.18	6.37	6.60	8.19
	$U - B$	0.17	0.12	0.44	0.16	0.12	0.44	0.16	0.12	0.44
	$B - V$	0.66	0.62	0.83	0.66	0.63	0.83	0.65	0.62	0.83
	$V - R$	0.36	0.34	0.45	0.36	0.34	0.45	0.36	0.34	0.45
Ström.	$u$	8.70	8.83	11.05	8.70	8.83	11.05	8.70	8.82	11.07
	$v$	7.74	7.90	9.91	7.74	7.90	9.91	7.74	7.90	9.93
	$b$	7.10	7.29	9.06	7.10	7.29	9.07	7.10	7.28	9.10
	$y$	6.70	6.91	8.58	6.70	6.91	8.58	6.70	6.91	8.60
	$u - v$	0.96	0.93	1.14	0.96	0.93	1.14	0.96	0.93	1.14
	$v - b$	0.64	0.61	0.85	0.64	0.61	0.85	0.64	0.61	0.85
	$b - y$	0.40	0.38	0.48	0.40	0.38	0.48	0.39	0.38	0.48
Tycho	$B_T$	7.55	7.71	9.68	7.55	7.71	9.68	7.55	7.71	9.70
	$V_T$	6.80	7.01	8.71	6.80	7.01	8.71	6.80	7.01	8.73
	$B_T - V_T$	0.74	0.70	0.97	0.74	0.70	0.97	0.74	0.70	0.97

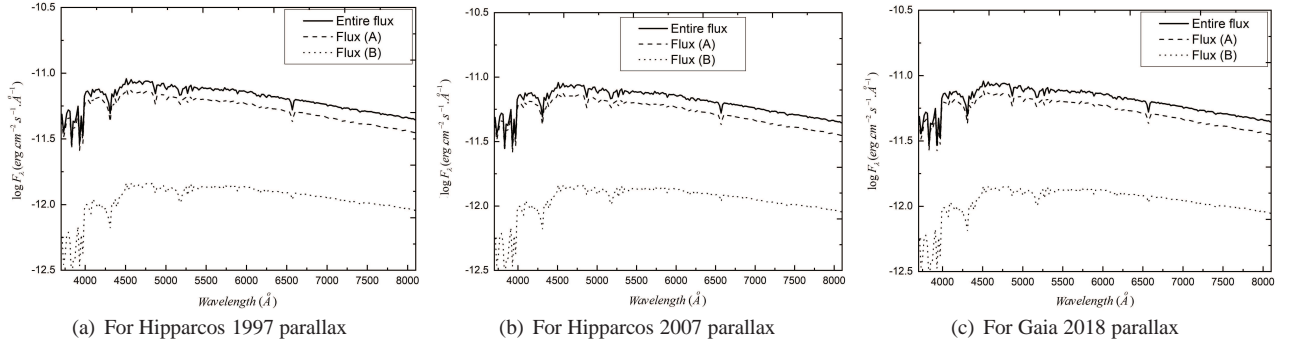


**Fig. 3** The entire flux and individual synthetic SEDs of the binary system HIP 43766 relying on Kurucz blanketed models (Kurucz 1994) (ATLAS9).

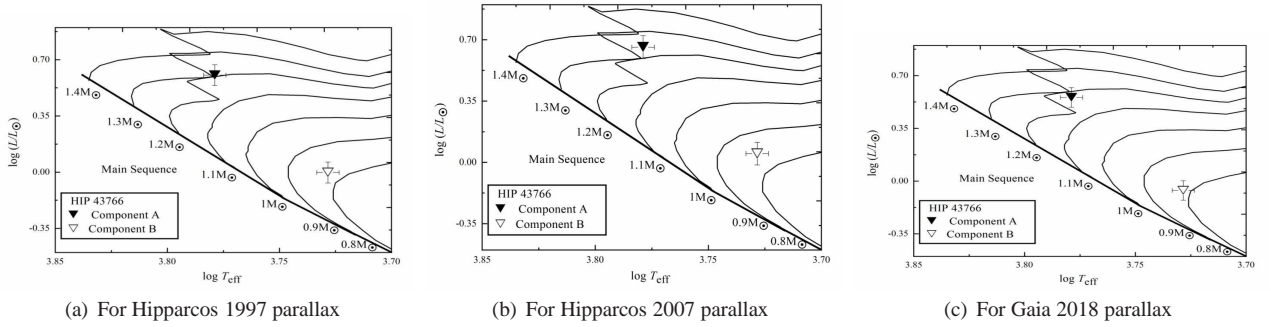


**Fig. 4** The evolutionary tracks of both components of HIP 43766 on the H-R diagram with varying masses (0.8, 0.9, ..., 1.4  $M_{\odot}$ ). The evolutionary tracks are adopted from Girardi et al. (2000).

**Table 9** Comparison between the Observational and Synthetic Magnitudes and Color Indices for the HIP 43766 System

Filter	Observed [mag]	Synthetic (This work) [mag]		
		$\pi_{\text{Hip1997}}$	$\pi_{\text{Hip2007}}$	$\pi_{\text{Gaia2018}}$
$V_J$	6.73	$6.73 \pm 0.03$	$6.73 \pm 0.03$	$6.73 \pm 0.03$
$(B - V)_J$	6.73	$6.73 \pm 0.03$	$6.73 \pm 0.03$	$6.73 \pm 0.03$
$\Delta m$	1.686	1.678	1.683	1.678

Since the SED for the two components of our system is not observed, we should rely on other quantities as a reference for the best fit with the synthetic one. The Al-Wardat complex method for analyzing close visual binary systems is followed to get the best fit (Al-Wardat 2002). In this method, the magnitudes and color indices are utilized as a reference to ensure the reliability of the estimated quantities.

Following Al-Wardat (2002), the synthetic magnitudes are calculated from the synthetic SED using the following relationship

$$m_p = -2.5 \log \frac{\int P_p(\lambda) F_{\lambda,s}(\lambda) d\lambda}{\int P_p(\lambda) F_{\lambda,r}(\lambda) d\lambda} + Z P_p, \quad (12)$$

where  $m_p$  represents the synthetic magnitude of the pass-band  $p$ ,  $P_p$  is the dimensionless sensitivity function of the pass-band  $p$ , and  $F_{\lambda,s}(\lambda)$  and  $F_{\lambda,r}(\lambda)$  are the synthetic SEDs of the star being studied and the reference star (Vega

in this case), respectively. The zero points,  $Z$ , were taken from Apellániz (2007).

The most accurate physical properties of the system are obtained when we get the best synthetic SED. This will lead to synthetic magnitude and color index values that are consistent with those obtained from observations (<http://simbad.u-strasbg.fr/simbad>, SIMBAD catalog) within the error values.

Utilizing Equation (11), we calculate the entire flux of the system from the fluxes of the two components of the system and depending on the parallax of the system. The best-fit for the SED of the system is featured in Figure 3. Also, based on the physical properties listed in Table 7 which are obtained from the best-fit SED, we plot the stars on the stellar evolutionary tracks diagram by Girardi et al. (2000). This is displayed in Figure 4.

We have used three photometrical systems; Johnson:  $U, B, V, R, U - B, B - V, V - R$ ; Strömgren:  $u, v, b,$



**Table 10** Estimated Physical Parameters of Individual Components in the HIP 43766 System

Parameter	Unit	Comp. A	Comp. B
$T_{\text{eff}}$	[K]	$6010 \pm 70$	$5350 \pm 70$
$R$	$[R_{\odot}]$	$1.852 \pm 0.12$	$1.164 \pm 0.11$
$\log g$	[cgs]	$4.50 \pm 0.15$	$4.55 \pm 0.16$
$M_V$	[mag]	$3.36 \pm 0.13$	$4.95 \pm 0.14$
$M_{\text{bol}}$	[mag]	$3.24 \pm 0.13$	$4.76 \pm 0.14$
$M$	$[M_{\odot}]$	$1.21 \pm 0.08$	$0.85 \pm 0.09$
Sp. Type		F4	G4

$y$ ,  $u - v$ ,  $v - b$ ,  $b - y$  and Tycho:  $B_T$ ,  $V_T$ ,  $B_T - V_T$  (see Al-Wardat 2012). The magnitudes and color indices of the entire and individual components of HIP 43766 are shown in Table 8.

The observational magnitude, color index and magnitude difference as well as the synthetic ones are listed in Table 9. We realize there is a high consistency between this work and observations. This gives a good indication of the reliability of the estimated parameters for the individual components of the system based on parallax measurements.

We have estimated the physical parameters of each component in the system for the three values of parallaxes. Fortunately Al-Wardat’s method enables us to determine which parallax gives the correct values of the physical parameters. For binary stars, there are different methods to estimate the masses. For example, utilizing Kepler’s third law from Equation (1), we can estimate the dynamical mass sum. Also, Al-Wardat’s method enables us to estimate the masses of individual components by their positions in the Hertzsprung-Russell (H-R) diagram and evolutionary track.

Table 4 shows a comparison between dynamical mass sum of the system from the Mason work and this work, while Al-Wardat’s method gives a mass sum of  $2.06 M_{\odot}$  for  $\pi_{\text{Hip}1997}$ ,  $2.10 M_{\odot}$  for  $\pi_{\text{Hip}2007}$  and  $2.00 M_{\odot}$  for  $\pi_{\text{Gaia}2018}$ . It is very interesting to note that Al-Wardat’s mass sum is independent of the parallax value. From the comparison of dynamical masses with Al-Wardat’s mass sum, we realize that parallax measurement from Hipparcos 2007 gives a high difference between masses, but the parallax measurement of Hipparcos 1997 provides a good indication about the mass sum, as does Gaia 2018, but HIP 43766 has a large error value within Gaia measurements. We conclude that the best estimated physical parameters for individual components of the HIP 43766 system are for parallax measurement of Hipparcos 1997 which are listed in Table 10.

## 4 RESULTS AND DISCUSSION

There is a high consistency between the synthetic magnitudes and color indices and the observational ones (Table 9). This is an indication of the correctness of values

for the calculated parameters of the individual components of the system which are listed in Table 10.

Figure 4 depicts the positions of the system’s components on the evolutionary tracks of Girardi et al. (2000). It affirms that the primary component is more massive and more evolved than the secondary one.

The parameters of the system and the positions of the components on the evolutionary tracks indicate that the system consists of F5 and G5 subgiant stars. Such stars with the same fundamental parameters are most probably formed by fragmentation, where Bonnell & Bate (1994) concluded that fragmentation of a rotating disk around an incipient central protostar is possible, as long as there is continuing infall. Zinnecker & Mathieu (2001) also pointed out that hierarchical fragmentation during rotational collapse has been invoked to produce binaries and multiple systems.

Since the system has three different parallax values, we have calculated three values for the total dynamical mass for the system utilizing Equation (1). Moreover, Al-Wardat’s mass sum is independent of the parallax value and yields a total mass of  $2.0 M_{\odot}$ .

Figure 2 displays the modified orbit and acts as a comparison with the old one which is obtained by Mason (2000) following the Tokovinin method (Tokovinin 2016). The estimated new values of the orbital elements are listed in Table 3.

The best estimated physical parameters of individual components of the system are displayed in Table 10 for the parallax measurement  $\pi_{\text{Hip}1997}$ , because the dynamical total mass for parallax measurement of Hipparcos 1997 is very close to the value obtained from Al-Wardat’s mass sum.

We can predict a dynamical mass sum of the system by relying on Equation (1) (see for example Al-Wardat et al. 2014c). Using the estimated values of the period and semi-major axis listed in Table 3, and the average values of mass sum obtained from the Al-Wardat method ( $M_{\text{tot}} = 2.053 M_{\odot}$ ), we arrive at a dynamical parallax  $\pi_{\text{dyn.}} = 22.096 \pm 0.19$ . Note that this value is close to the parallax obtained by Hipparcos 1997.

## 5 CONCLUSIONS

In this paper, we analyzed the stellar system HIP 43677 to determine the properties of its two components. We applied recent data and methods developed by Al-Wardat (2002) (atmospheric modeling) and Tokovinin (2016) (dynamical modeling) to determine the physical properties and orbital solution for the system, respectively, with better accuracy than past studies. The physical and geometrical parameters of the system’s components are estimated depending on the best fit between the observational and synthetic SEDs, built using the atmospheric modeling

of the individual components and the system's orbital elements.

The spectral types of components of the system are F4IV and G4IV for the primary and secondary components, respectively.

The entire and individual synthetic magnitudes and color indices of the system are calculated for the three photometric systems and their corresponding filters. We suggested that the fragmentation process is the most probable mechanism for the formation of the system. Finally, a dynamical mass sum of the system is predicted.

**Acknowledgements** The authors thank Prof. Mashhoor Al-Wardat for suggesting the binary system and for fruitful discussion on the manuscript. The authors also thank Mr. Abdallah Hussein for his help in some calculations and Prof. Ahmed Al-Jamel for language editing. This work has made use of the Fourth Interferometric Catalogue of Binary Stars, SIMBAD database, Sixth Catalog of Orbits of Visual Binary Stars, ORBITX code and Al-Wardat's complex method for analyzing close visual binary and multiple systems with its codes. The authors express sincere thanks to the anonymous referee for his critical comments on the manuscript.

## References

- Al-Wardat, M. 2002, *Bull. Spec. Astrophys. Obs.*, 53, 51  
 Al-Wardat, M. 2012, *PASA*, 29, 523  
 Al-Wardat, M. A., El-Mahameed, M. H., Yusuf, N. A., et al. 2016, *RAA (Research in Astronomy and Astrophysics)*, 16, 166  
 Al-Wardat, M., Balega, Y. Y., Leushin, V., et al. 2014a, *Astrophysical Bulletin*, 69, 58  
 Al-Wardat, M., Balega, Y. Y., Leushin, V., et al. 2014b, *Astrophysical Bulletin*, 69, 198  
 Al-Wardat, M., Docobo, J., Abushattal, A., & Campo, P. 2017, *Astrophysical Bulletin*, 72, 24  
 Al-Wardat, M., Widyan, H., & Al-thyabat, A. 2014c, *PASA*, 31, 1  
 Apellániz, J. M. 2007, in the *Future of Photometric, Spectrophotometric and Polarimetric Standardization*, 364, 227  
 Balega, Y. Y., & Tikhonov, N. 1977, *Soviet Astronomy Letters*, 3, 272  
 Bonneau, D., Balega, Y., Blazit, A., et al. 1986, *A&A*, 65, S27  
 Bonnell, I. A., & Bate, M. R. 1994, *MNRAS*, 269, L45  
 Collaboration, G., & et al. 2018, *VizieR Online Data Catalog*  
 Duquennoy, A., & Mayor, M. 1992, *Binaries as Tracers of Stellar Formation* (Cambridge Univ. Press)  
 ESA. 1997, *The Hipparcos and Tycho Catalogues* (ESA)  
 Fabricius, C., Høg, E., Makarov, V., et al. 2002, *AJ*, 384, 180  
 Fabricius, C., & Makarov, V. 2000, *A&A*, 356, 141  
 Fu, H.-H., Hartkopf, W., Mason, B., et al. 1997, *AJ*, 114, 1623  
 Gili, R., & Prieur, J.-L. 2012, *Astron. Nachrichten*, 333, 727  
 Girardi, L., Bressan, A., Bertelli, G., & Chiosi, C. 2000, *A&A*, 141, S371  
 Gray, D. F. 2005, *The Observation and Analysis of Stellar Photospheres* (Cambridge Univ. Press)  
 Hartkopf, W., McAlister, H., & Franz, O. 1992, *AJ*, 104, 810  
 Hartkopf, W., McAlister, H., Mason, B., et al. 1994, *AJ*, 108, 2299  
 Hartkopf, W., McAlister, H., Mason, B., et al. 1997, *AJ*, 114, 1639  
 Hartkopf, W., Mason, B., McAlister, H., et al. 2000, *AJ*, 119, 3084  
 Høg, E., Fabricius, C., Makarov, V. V., et al. 2000, *A&A*, 355, L27  
 Kurucz, R. 1994, *Solar Abundance Model Atmospheres for 0,1,2,4,8 km s<sup>-1</sup>*, Smithsonian Astrophysical Observatory, 19  
 Labeyrie, A. 1970, *A&A*, 6, 85  
 Lallement, R., Vergely, J. L., Valette, B., et al. 2014, *A&A*, 561, A91  
 Lang, K. 1992, *Astrophysical Data: Planets and Stars*, 132ff  
 Masda, S., Docobo, J., Hussein, A., et al. 2019a, *Astrophysical Bulletin*, 74, 464  
 Masda, S. G., Al-Wardat, M. A., & Pathan, J. K. M. K. 2018, *RAA (Research in Astronomy and Astrophysics)*, 18, 072  
 Masda, S. G., Al-Wardat, M. A., & Pathan, J. M. 2019b, *RAA (Research in Astronomy and Astrophysics)*, 19, 105  
 Mason, B. 2000, *IAUDS, Inf. Circ.*, 141  
 Mason, B. D., Hartkopf, W. I., Miles, K. N., et al. 2018, *AJ*, 155, 215  
 Mason, B., Hartkopf, W., Raghavan, D., et al. 2011, *AJ*, 142, 176  
 McAlister, H.A. and Fekel, F. 1980, *Astrophys. J. Suppl. Ser.*, 43, 327  
 McAlister, H. 1978, *Astrophys. J.*, 225, 932  
 McAlister, H., & DeGioia, K. 1979, *AJ*, 228, 493  
 McAlister, H., Hartkopf, W., & Franz, O. 1990, *AJ*, 99, 965  
 McAlister, H., Hartkopf, W., Hutter, D., & Franz, O. 1987, *AJ*, 93, 688  
 McAlister, H., Hartkopf, W., Sowell, J., Dombrowski, E., & Franz, O. 1989, *Astron. J.*, 97, 510  
 McAlister, H., Hendry, E., Hartkopf, W., Campbell, B., & Fekel, F. 1983, *Astrophys. J. Suppl. Ser.*, 51, 309  
 Roberts Jr, L., & Mason, B. 2017, *MNRAS*, 473, 4497  
 Sürgit, D., Erdem, A., Engelbrecht, C. A., & Marang, F. 2020, *MNRAS*, 493, 2659  
 Tokovinin, A. 1982, *Sov. Astron. Lett.*, 8, 187  
 Tokovinin, A. 1983, *Sov. Astron. Lett.*, 9, 293  
 Tokovinin, A. 1992, *HA McAlister & WI Hartkopf*, (ASP, San Francisco), 32, 573  
 Tokovinin, A. 2016, *AJ*, 152, 11  
 Van Leeuwen, F. 2007, *A&A*, 474, 653  
 Zinnecker, H., & Mathieu, R. D. 2001, in *Symposium-International Astronomical Union*, 200 (Cambridge Univ. Press), 1